e-ISSN: 2582-5208
International Research Journal of Modernization in Engineering Technology and Science
Volume:03/Issue:06/June-2021 Impact Factor- 5.354 www.irjmets.com

STATIC AND DYNAMIC ANALYSIS OF ROBOTIC ARM WITH A GRIPPER

Samir Chakravarti*1, Souvik Sarkar*2, Suvro Mukherjee*3, Moinak Biswas*4

*1Assistant Professor, Department of Mechanical Engineering, Kalyani Government Engineering College, Kalyani, West Bengal, India.

*2,3,4Student, Department of Mechanical Engineering, Kalyani Government Engineering College, Kalyani, West Bengal, India.

ABSTRACT

This paper is focussed on static and dynamic analysis of a 5 degrees of freedom robotic arm with a gripper which are performed under ANSYS workbench in the analysis system of static structural and rigid dynamics. The entire robotic arm and its griper are designed with the help of SolidWorks. The load carrying capacity of each component of the robotic arm and the gripper is determined by observing the maximum stress induced due to applied force in each component of the robotic arm and gripper. The weakest parts of each component of the robotic arm are also obtained by observing their stress distribution through ANSYS simulation tool. An optimum design of the robotic arm and its gripper is achieved after the evaluation of the results of statics and dynamic analysis.

Keywords: Robotic Arm, Gripper, ANSYS, Solidworks, Static, Dynamic.

I. INTRODUCTION

Robot is a machine which can execute various tasks repeatedly and its precision is also very good. Thereby it is mainly used in the manufacturing industry for producing good quality products in less time with precision. There are many functions like collecting information and conducting studies about the hazardous sites which are too risky for humans to reach those places. Robots are used to minimize human interference almost 50 percent [1].A geometric approach to solve the unknown joint angles required for the autonomous positioning of a robotic arm was used by a complex mathematical process. The complexity of the mathematical process was reduced using basic trigonometry in the modelling of the robotic arm. This modelling and analysis approach was tested using a five-degree-of-freedom arm with a gripper style end effector mounted to an iRobot Create mobile platform [2]. Ferdinand et al. [3] showed design, modelling and analysis of a robotic arm and it aimed to minimize weight in order to fulfil the demands of the manufacturing industry. Omijeh and Uhunmwangho [4] revealed the fact that man would always want to stay attached to safety precautions at the workplace and even in its environment, in order to handle some specific tasks, like sending the robotic vehicle to dangerous environments to obtain samples for various chemical studies. Iqbal et al. [5] described the kinematic model of a six DOF robotic arm and analysed its workspace and stated that it was possible to make a model where the manipulator can be controlled to achieve any reachable position and orientation in an environment. They designed a robotic gripper and showed that the robotic gripper behaves like an end effector of a robot mechanism. Grippers are utilized in regions that contain risky responsibilities along with area exploration, high-temperature welding, dealing with radioactive materials, defusing bombs, mines, and exploring shipwrecks etc. The design of the robot gripper provides an active research area as it is highly used in automation, especially for high-precision micro-machining [6]. Robot grippers often encounter difficulties performing complex manipulation tasks in unstructured environments. Nowadays special robot gripper has been coming which are challenging the universal grasp capability of robot grippers [7]. On the basis of these models, a problem based upon structural and multi-objective optimization is validated in static configuration of gripper [8]. The applicability and proposed approach in robotic motion has been proved by comprehensive experimental results [9].

In this work, the objective is to make a model of robotic arm of five degrees of freedom with a gripper in SolidWorks 2020.The statics analysis of the robotic arm and the gripper is aimed to determine the maximum load carrying capacity by observing the maximum stress induced due to applied forces at the different components of the robotic arm and the gripper. The weakest portion of each component of the robotic arm and gripper is observed from their stress distribution which is obtained through ANSYS simulation tool. The dynamics forces induced due to rotary motion of the joints of the robotic arm and the gripper are to be obtained under dynamic analysis.

II. MODELING AND ANALYSIS

The design of the robotic arm with a gripper made with the help of SolidWorks 2020. The assembly of the model of the robotic arm with a gripper is shown in figure 1.

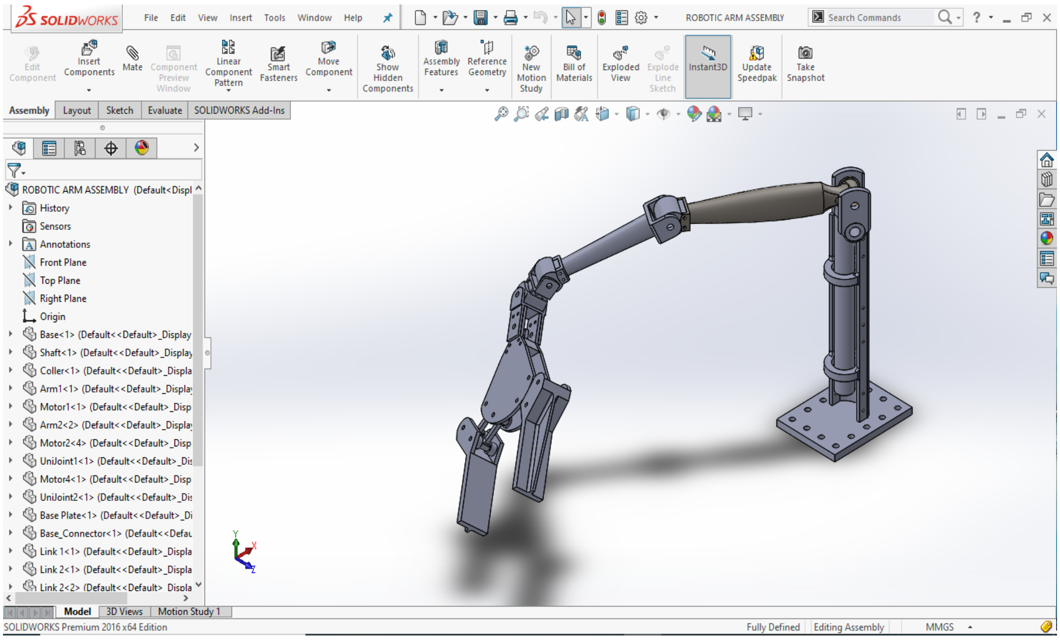

Figure 1: Model of the robotic arm

The different parts of the robotic arm are base, shaft, collar, arm 1, arm 2, universal joint and gripper. All of these parts are shown in figure 2.

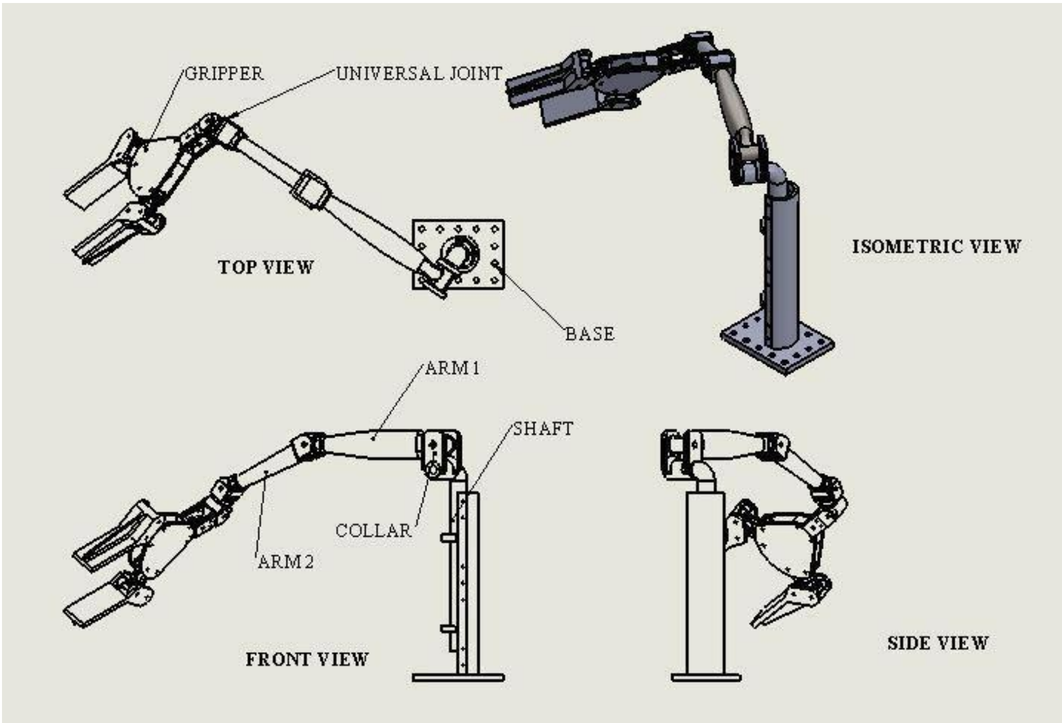

Figure 2: Different parts of robotic arm

There are few assumptions pertaining to the design and analysis of the robotic arm and gripper. The assumptions are given below-

1) The material is homogeneous and isotropic.

2) During kinematics and dynamics analysis the components of the robotic arm are rigid.

3) All the joints of the robotic arm and gripper are frictionless.

e-ISSN: 2582-5208
International Research Journal of Modernization in Engineering Technology and Science
Volume:03/Issue:06/June-2021 Impact Factor- 5.354 www.irjmets.com

The joint between the base and the shaft is a twisting joint and the joint between the collar and shaft is fixed. Further the collar is connected to arm 1 by a revolute joint. Also the arm 1 and arm 2 are connected by a revolute joint among themselves. The gripper is connected to arm 2 with a universal joint. Many materials could be chosen the design such as Iron or Iron based Alloys. The material may be casted [11] for the appropriate design of proposed robotic arm. For the present study, we have considered structural steel for the component of the robotic arm and gripper and the properties are given in table 1.

Table 1: Material properties of structural steel S690Q

Properties	Values
Density	7850 Kg/m^3
Young Modulus	210 GPa
Poisson's Ratio	0.3
Bulk Modulus	175 GPa
Shear Modulus	81 GPa
Tensile Strength	770 MPa
Allowable Tensile Stress	470 MPa

III. RESULTS AND DISCUSSION

Statics Analysis of Robotic Arm

Static Structural of ANSYS analysis system has been evolved to carry out the essential calculations of static loading on different parts of the robotic arm. Force is applied to one end of the part of the robotic arm and the other end of the part of the robotic arm is fixed. The arms of the robotic arm behave like a cantilever beam. The stress of a beam is calculated from the equation [9].

$$\sigma_b = \frac{M}{I} y \quad (1)$$

The analysis of the stress generated due to applied force is done separately for each component of the robotic arm. In the statics part, the induced stresses have been estimated on each part of the robotic arm due to an external load acting on each part of the robotic arm. In each part of the robotic arm, the applied forces are given in successively increased values with respect to time. The load carrying capacity of the various components of the robotic arm can be determined with the help of static analysis.

Stress Results of Base and Shaft

The static analysis of base and shaft is performed with the help of ANSYS 2020 under the analysis system of static structural. The pictorial representation of applied force on the base and shaft is shown in figure 3 and their corresponding stress distribution is shown in figure 4.

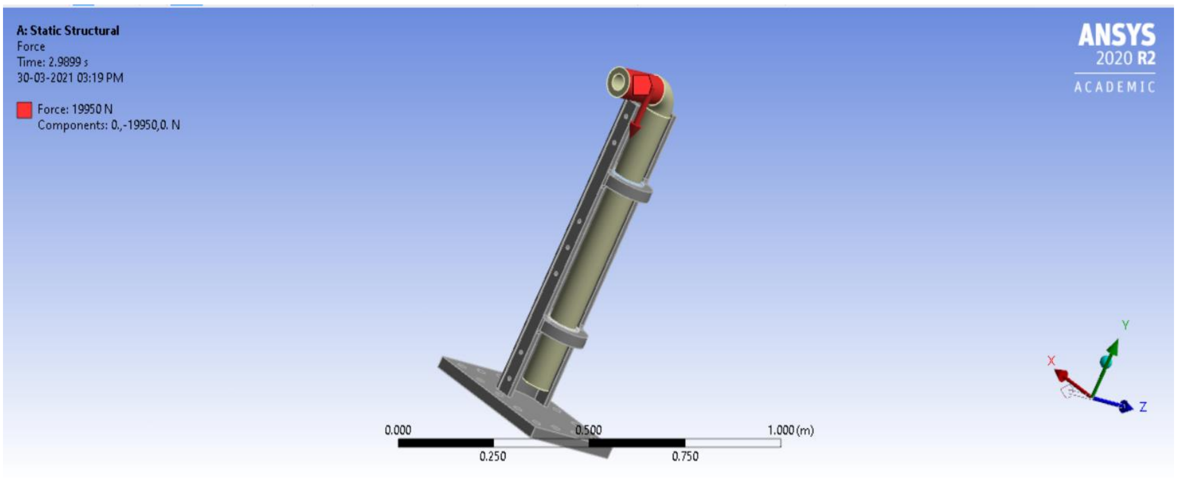

Figure 3: Force acting on base

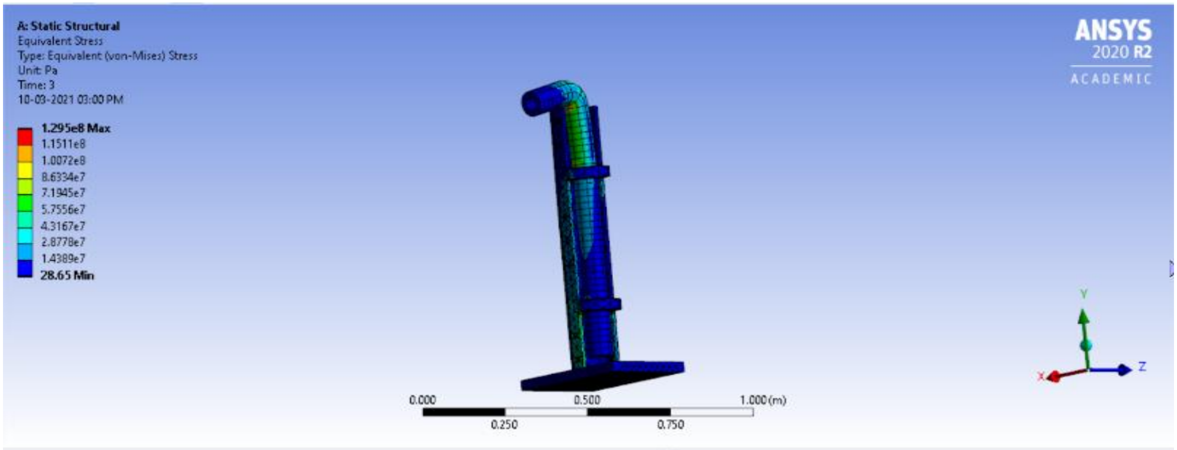

Figure 4: Stress results of base

Table 2: Maximum stress values of base due different applied force

Steps	Time [sec]	Force [N]	Maximum Stress [Pa]
1	1	10000	6.48E+07
2	2	15000	9.71E+07
3	3	20000	1.30E+08

The bottom of the base is fixed. The stress results are obtained by applying force at a particular point of the shaft as shown in figure 3. The maximum stress during 10000 N, 15000N and 20000N force are 6.48E+07 Pa, 9.71E+07 and 1.30E+08 Pa respectively. The maximum stress occurs at the bend of the shaft due to the effect of stress concentration at the bend. The minimum stress occurs at the bottom of the base where it is fixed as strain is minimum at the fixed end which is observed from figure 4. Therefore, from the static analysis of the base the safe load of the base is obtained to be 20000N and it is observed that the bend of the shaft is the weakest portion of the shaft.

Stress Results of Collar

The static analysis of the collar is performed with the help of ANSYS 2020. The direction and point of application of force applied on the collar is shown in figure 5. The stress result of collar obtained by the analysis is shown in figure 6.

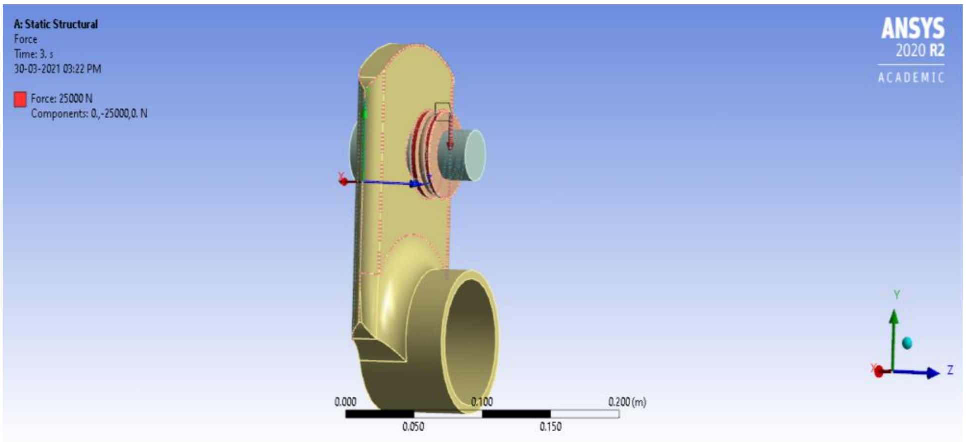

Figure 5: Force acting on collar

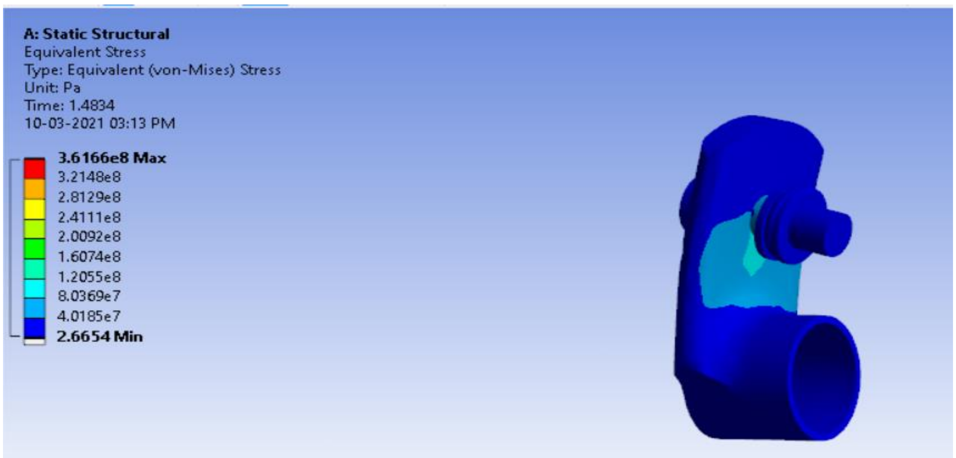

Figure 6: Stress results of collar

Table 3: Maximum stress values of collar due different applied loads

Steps	Time [sec]	Force [N]	Maximum Stress [Pa]
1	1	1500	2.74E+08
2	2	2500	4.56E+08
3	3	3000	4.56E+08

The inner circumference of the collar is fixed. The point of application and direction of applied force at the collar is shown in figure 5. The static analysis is done on the half portion of the collar due to its symmetry and this helps to reduce the memory to solve the numerical equations in Ansys. The maximum stress values for 1500N, 2000N and 3000N forces are 2.74E+08 Pa, 4.56E+08 Pa and 4.56E+08 Pa respectively. The maximum stress i.e. 5.56E+08 Pa is less than the maximum allowable stress i.e. 4.70E+08 Pa of the material. Therefore, from this observation, the safe load for the half portion of the collar is found to be 3000 N. Therefore, the safe load for the entire collar is (2 x 3000) N i.e. 6000 N.

Stress Results of Arm 1

The static analysis of arm 1 is performed with the help of ANSYS 2020 under the analysis system of static structural. The pictorial representation of applied force on the arm 1 is shown in figure 7 and their corresponding stress distribution is shown in figure 8.

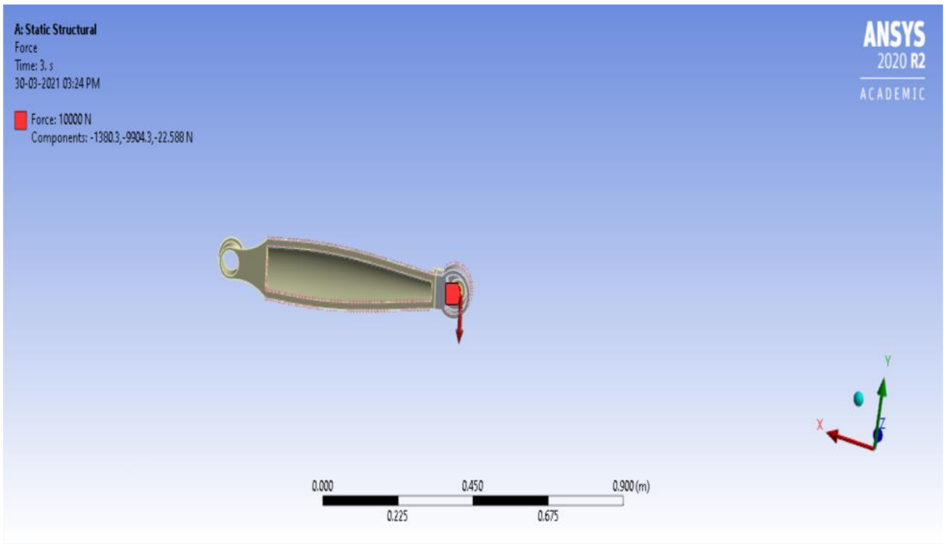

Figure 7: Force acting on arm 1

e-ISSN: 2582-5208
International Research Journal of Modernization in Engineering Technology and Science
Volume:03/Issue:06/June-2021 Impact Factor- 5.354 www.irjmets.com

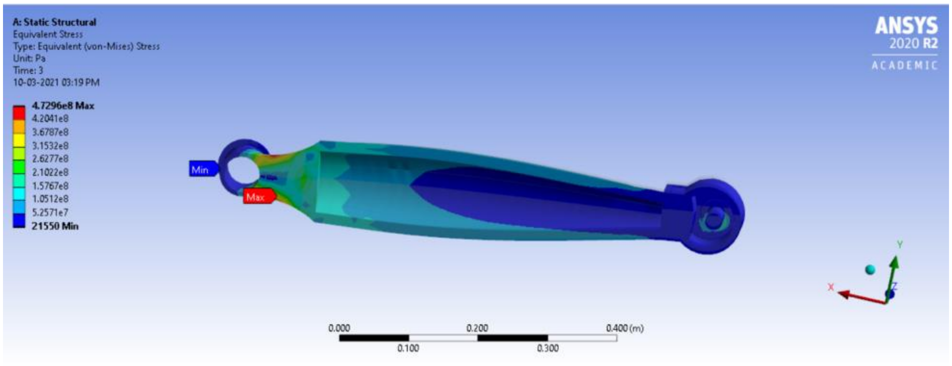

Figure 8: Stress results of arm 1

Table 4: Maximum stress values of arm1 due different applied loads

Steps	Time [sec]	Force [N]	Maximum Stress [Pa]
1	1	3000	1.63E+08
2	2	5000	2.36E+08
3	3	10000	4.73E+08

The point of application and direction of applied force on arm 1 is shown in figure 7. In this case also the half portion of arm 1 is statically analysed due to its symmetry and to reduce the memory to solve the numerical equations in Ansys. The stress values for 3000N, 5000N and 10000N are 1.63E+08 Pa, 3.36E+08 Pa and 4.73E+08 Pa respectively. The maximum stress and minimum stress are observed at the fillet section and at the fixed end of the arm1 respectively which can be observed from figure 8. The applied load 10000 N is quite high and not safe as it induces maximum stress of 4.73E+8 Pa which is higher than the maximum allowable stress of the material i.e. 4.7E+8. So, it is found that 5000 N is safe for the half portion of the arm1. Therefore, the safe load of arm1 is (2 x 5000) N i.e. 10000 N.

Stress Results of Arm 2

The static analysis of Arm 2 is performed with the help of ANSYS 2020. The direction and point of application of force applied on arm 2 is shown in figure 9. The stress result of arm 2 obtained by the analysis is shown in figure 10.

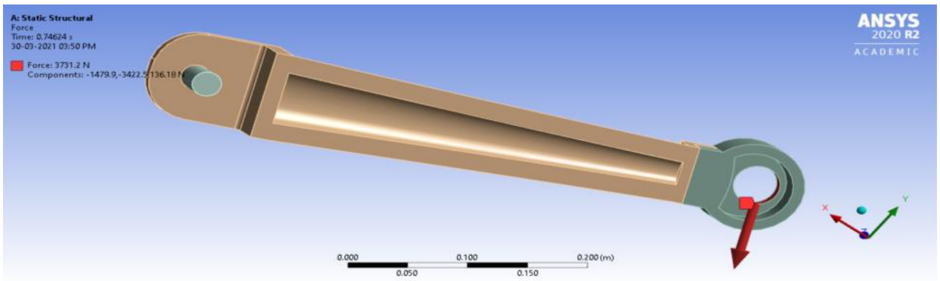

Figure 9: Force acting on arm 2

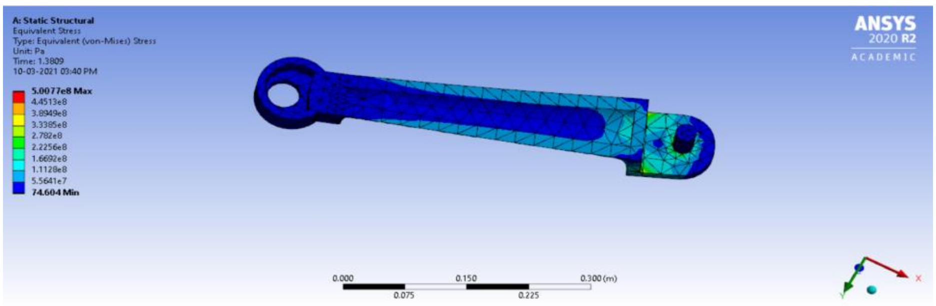

Figure 10: Stress results of arm 2

Table 5: Stress values of arm2 due different applied loads

Steps	Time [sec]	Force [N]	Maximum Stress [Pa]
1	1	5000	4.65E+08
2	2	6000	5.58E+08

The point of application and direction of force on arm 2 is shown in figure 9. In this case also the half portion of arm 2 is statically analysed due to its symmetry and to reduce the memory to solve the numerical equations in Ansys. Applied forces of 5000 N and 6000 N are given at 1 second and 2 seconds respectively. The maximum stress during 6000 N load is very high and a high stress of 5.58E+08 Pa is generated which is higher than the maximum allowable stress of the material i.e. 4.7E+08 Pa. Although the maximum stress induced for the 5000 N load is very near to maximum allowable stress of the material, it is considered as the safe load. Therefore, maximum load can be applied to arm 2 is (2 x 5000) N i.e. 10000 N.

From the entire static analysis of the robotic arm, it is found that the weakest part of the mechanism is its collar which is capable of carrying a maximum 6000 N load safely. And the strongest part of the mechanism is its base and shaft which is capable of carrying 20000N safely.

Dynamic Analysis of Robotic Arm

There are two revolute joints in the robotic arm between arm 1 and collar and between arm 2 and arm1. The revolute joint between arm 1 and collar is named 'Revolute joint 1' and the revolute joint between arm 2 and arm 1 is named 'Revolute joint 2'. The joint between the shaft and base is the twisting joint. The variation of applied angular velocities of different joints of the robotic arm with respect to time is shown in chart 1. When the rotation of joints of the robotic arm is anti-clock wise, the angular velocity of the joints is taken positive and when the rotation of the joints of the robotic arm is clockwise, the angular velocity of the joints is taken negative. The maximum applied angular velocity of revolute joint 1 is 1 RPM. The rotation of revolute joint 1 is given clockwise. The maximum applied angular velocity of the twisting joint is 2 RPM. The rotation of the twisting joint is given anti-clockwise. There is no angular velocity provided at the revolute joint 2. Force is induced in revolute joint 1 due to the rotation of revolute joint 1 and twisting joint. The induced force in revolute joint 1 is determined and its variation with respect to time can be observed from chart 2.

It is observed that the average force acting at revolute joint 1 is nearly 400 N. Fluctuation of dynamic forces is observed in revolute joint 1 as the robotic arm is not dynamically balanced. The entire robotic arm is operated at a low speed which leads to very less fluctuation of dynamic force. Therefore, very low vibration can take place in the robotic arm.

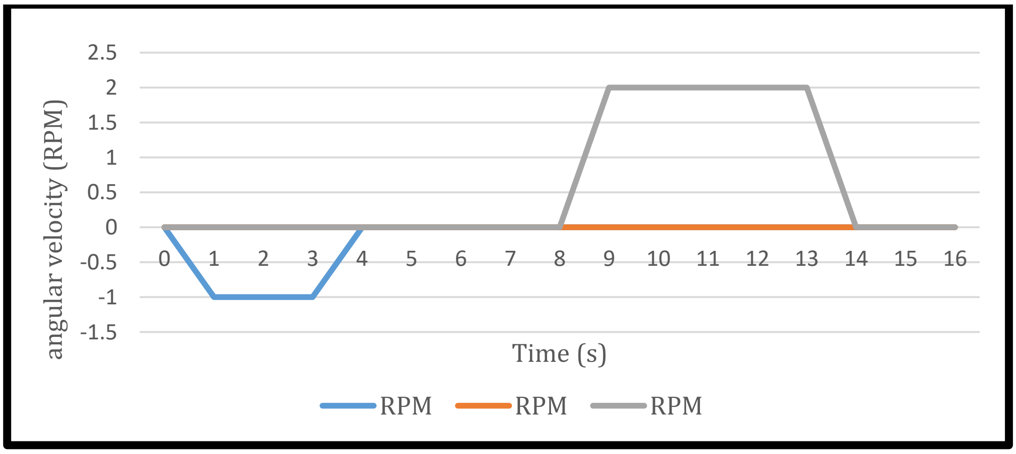

Chart 1: Input angular velocities to the joints

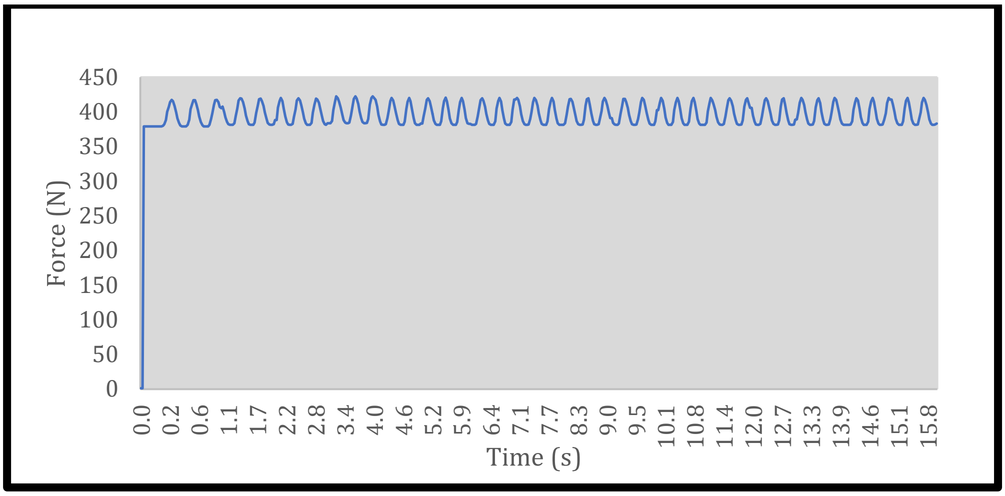

Chart 2: Force at the revolute joint 1

Dynamics Analysis of Gripper

The gripper works on the mechanism of the slider crank. The jaws of the griper is opened by retracting the slider and the jaws of the slider is closed by extending the slider. Displacement is provided at the slider so that it can open or close the jaws. The slider is completely retracted when its displacement is 4.00E-02 m which indicates the jaws are closed and the slider is completely extended when its displacement is zero which indicates the jaws are open. The values of displacement of the slider of the gripper are shown in table 6.

Forces of equal magnitude are provided on both the jaws of the gripper. The force is provided in the opposite direction of the normal vector of the jaw surface. The direction of the force is constant for each jaw but the magnitude is changed with respect to time. The magnitude of force with respect to time is shown in table 6. After providing forces at both the jaws and displacement at the slider of the gripper, induced force and moment of the joint of the crank is determined. The joint of the crank where induced force is determined is shown on figure 11. The variation of this induced force at the joint of the crank with respect to time is shown graphically in chart 3.

Table 6: Applied force at each jaws and displacement of the slider of the gripper

Time [sec]	Applied Force at Each Jaws [N]	Displacement of Slider [m]
1	1000	1.00E-02
2	1000	2.00E-02
3	2000	3.00E-02
4	2000	4.00E-02
5	0	4.00E-02
6	0	0
7	3000	0
8	3000	0
9	3000	0
10	0	2.00E-02
11	0	4.00E-02
12	4000	4.00E-02
13	4000	0
14	4000	2.00E-02

15	4000	4.00E-02
16	0	4.00E-02
17	0	0
18	5000	0
19	5000	4.00E-02
20	5000	0

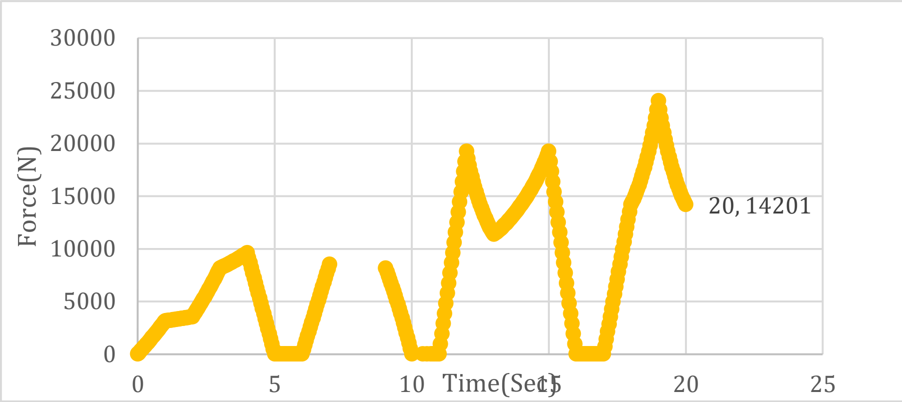

Chart 3: Time vs total force at joint of crank of gripper

From chart 3 it can be observed that the total force at the joint ranges between 0 to 25000N. The maximum induced force is observed at about 18 second time.

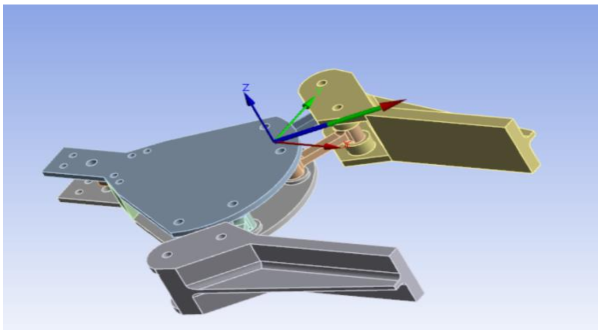

Figure 11: Force acting at the joint of crank of the gripper

Moment acting on the joint of the gripper crank is ranged from 0 to 650 N-m. The maximum approximate moment of 650 N-m is observed at about 18 second. It is observed that the variations of both the induced force and moment of the joint of the gripper crank with respect to time are the same. The joint location where the induced moment is determined is shown in Figure 12.

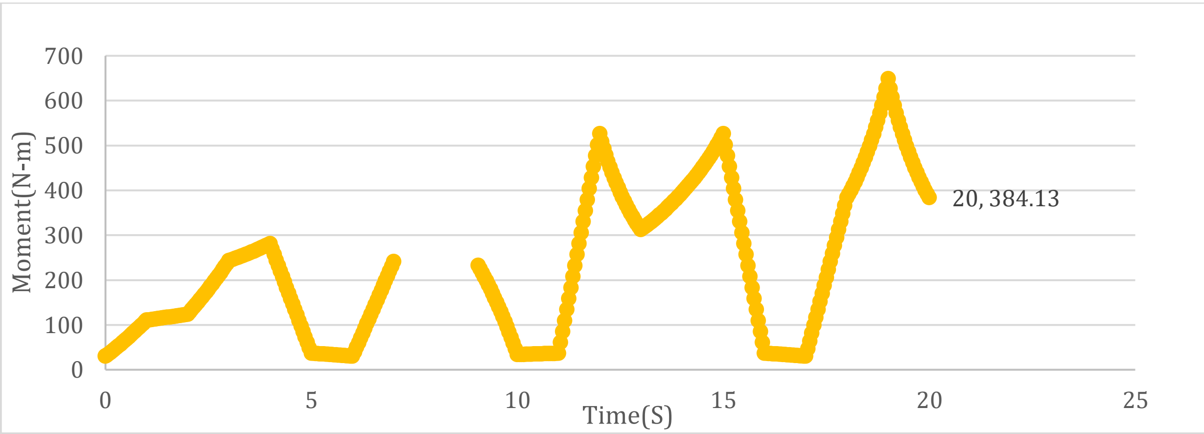

Chart 4: Time vs moment of the joint of gripper crank

e-ISSN: 2582-5208
International Research Journal of Modernization in Engineering Technology and Science
Volume:03/Issue:06/June-2021 Impact Factor- 5.354 www.irjmets.com

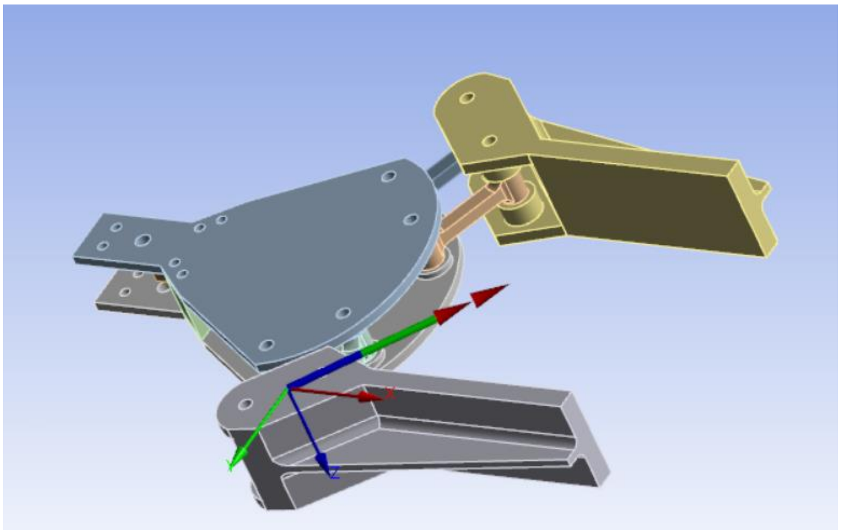

Figure 12: Moment acting at the joint of crank of gripper

Statics Analysis of the Crank of Gripper

In the entire dynamic analysis of the gripper it was observed that high force and moment are generated at the joint of the gripper crank. To ensure whether the crank is able to withstand these force and moment, static analysis is done. The values of applied force and moment at the joint of the crank are given in table 7.

Table 7: Maximum stress induced due to applied force and moment on the gripper crank

Time [s]	Applied Moment [N-m]	Applied Force [N]	Maximum Stress Induced [Pa]
1	100	5000	1.17E+07
2	200	10000	2.34E+07
3	300	15000	3.51E+07
4	400	20000	4.68E+07
5	500	25000	5.85E+07

The moment is applied in anticlockwise direction at the joint of the gripper crank. The location of the applied moment at the crank is shown in figure 13. The force is applied radially outwards to the direction of the gripper joint as shown in figure 14.

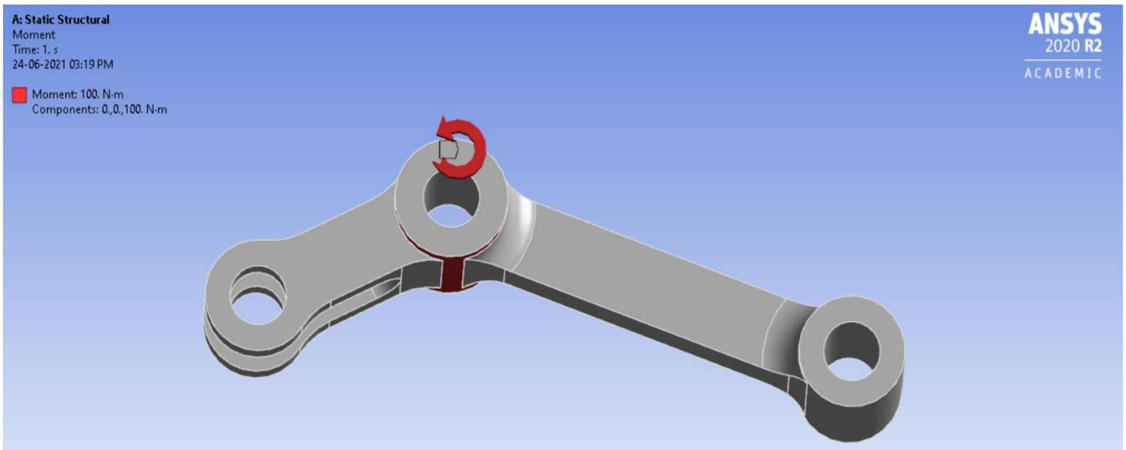

Figure 13: Applied moment on gripper crank

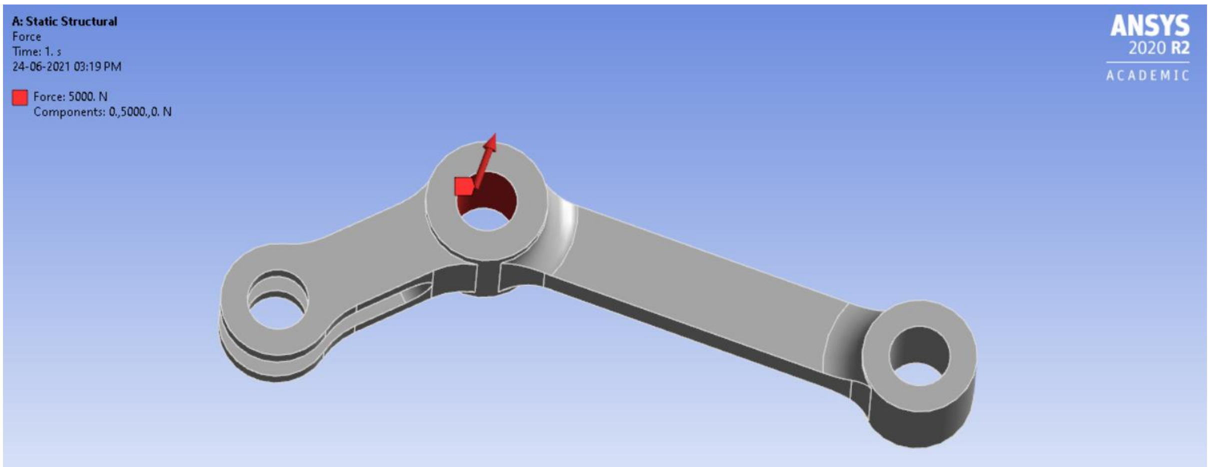

Figure 14: Applied force on the gripper joint

The induced stress in the gripper crank due to applied force and moment is determined. The maximum stress i.e. 5.85E+07 Pa is observed at 5 seconds time as shown in table 7. The allowable stress of the gripper material is 4.7E+08 Pa. The induced maximum stress is very less than the allowable stress of gripper material. Therefore, the applied force and applied moment can be easily with stand by the crank. The location of maximum induced stress and the distribution of induced stress can be observed from figure 15.

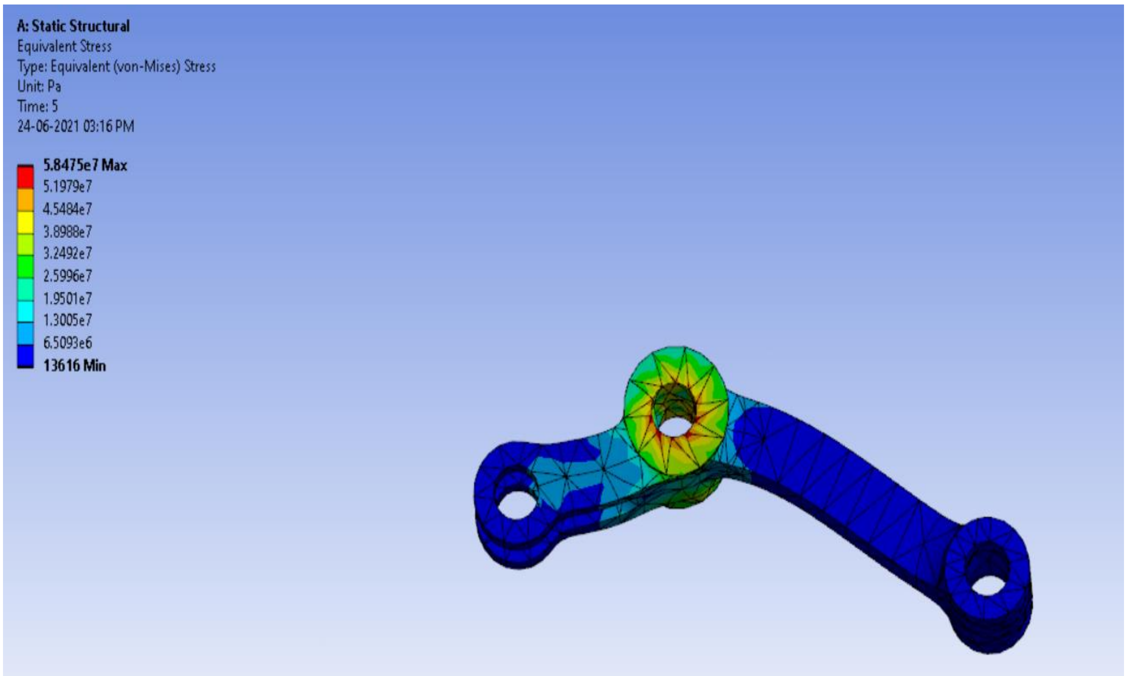

Figure 15: Stress result of gripper crank

IV. CONCLUSION

In the statics part, forces are applied on the bodies of the robotic arm and gripper which induce stress on those bodies. The behaviour of the body upon applied load is analysed by computing its stress. The collar part can carry a maximum 6000 N load safely and it is the weakest part of the robotic arm. The base and shaft can carry 20000 N force safely and it is the strongest part of the entire robotic arm. The arm 1 can carry 5000 N force safely and its maximum stress is observed at its fillet section. A safe load of 5000 N can be carried by arm 2 as well and the maximum stress of arm 2 is observed at the potion where it is connected with arm1. The average force acting at revolute joint 1 is nearly 400 N during the dynamic analysis of the robotic arm. Therefore, from these analyses, it is observed that the design of the robotic arm is safe for the above mentioned static loads and given angular velocities at the joints of the robotic arm. Each jaw of the gripper can easily withstand 5000 N loads simultaneously. That means total (5000 x 2) N i.e. 10000 N force can be withstand by the gripper.

V. REFERENCES

[1] R. Nair, “Design of a Robotic Arm for Picking and Placing an Object Controlled Using LabVIEW by Shyam”, International Journal of Scientific and Research Publications, Volume 2, Issue 5, May 2012.

[2] K.E. Clothier and Shang Y, “A geometric approach for robotic arm kinematics with hardware design, electrical design and implementation”, Journal of Robotics, Article ID 984823, Vol. 2010.

[3] P. Ferdinand, O. Joseph, Dr. K. Udayakumar, “Design, Modelling and Analysis of Industrial Robotic Arm Minimizing Weight and Capital Invested”, S.R.M University, June 2020.

[4] B. O. Omijeh and R. Uhunmwangho, “Design Analysis of a Remote Controlled ‘Pick and Place’ Robotic Vehicle”, International Journal of Engineering Research and Development, Volume 10, 5 May 2014, PP.57-68.

[5] J. Iqbal, R. Islam, and H. Khan, “Modelling and Analysis of a 6 DOF Robotic Arm Manipulator”, Canadian Journal on Electrical and Electronics Engineering Vol. 3, No. 6, July 2012.

[6] R. Dutta, S. Pradhan, and B. Bhattacharya, “Analysis and Design Optimization of a Robotic Gripper Using Multi-Objective Genetic Algorithm”, February, 2015.

[7] A. Mo and W. Zhang “Pin Array Hand: A Universal Robot Gripper with Pins of Ellipse Contour”, December 2017.

[8] A. Hassan and M. Abomoharam, “Modelling and design optimization of a robot gripper mechanism”, Robotics and Computer–Integrated Manufacturing, December 2016.

[9] A. R. J. Almusawi, L. C. Dülger and S. Kapucu, “A New Artificial Neural Network Approach in Solving Inverse Kinematics of Robotic Arm (Denso VP6242)”, Computational Intelligence and Neuroscience, Volume 2016, Article ID 5720163, July 2016.

[10] S. Timoshenko, “Strength of Materials: Elementary Theory and Problem”, 3rd Edition, Vol. 1.

[11] S. Chakravarti, S. Sen, and A. Bandyopadhyay, “A study on solidification of large iron casting in A thin water-cooled copper mould,” Mater. Today, vol. 5, no. 2, pp. 4149–4155, 2018.

[12] J. Narayan, S. Mishra, Gaurav Jaiswal, S. K. Dwivedy, “Novel design and kinematic analysis of a 5- DOFs robotic arm with three-fingered gripper for physical therapy”, Materials Today: Proceedings, April 2020.

[13] ANSYS Fluent – Release 20, Fluent Theory Guide, ANSYS Inc, <www.ansys.com>.

[14] Wen K and Gosselin C., “Static Model Based Grasping Force Control of Parallel Grasping Robots with Partial Cartesian Force Measurement”, IEEE/ASME Transactions on Mechatronics, May 2021.

[15] Nag, B. Menzies and S. C. Mukhopadhyay, “Performance analysis of flexible printed sensors for robotic arm applications”, Sensors and Actuators A: Physical, April 2018.